Calculation of the magnetization of the layered III-VI diluted magnetic semiconductor $Ga_{1-x}Mn_xS$

C. Fuller, A. Douglas, J. Garner, and T. M. Pekarek
Department of Chemistry and Physics, University of North Florida, Jacksonville, Florida 32224

I. Miotkowski and A. K. Ramdas
Department of Physics, Purdue University, West Lafayette, Indiana 47907

(Received 12 October 2001; revised manuscript received 8 February 2002; published 10 May 2002)

The magnetization of a compound belonging to a new class of diluted magnetic semiconductors (DMS) was calculated. The magnetization of the III-VI DMS, $Ga_{1-x}Mn_xS$, was found for the small x regime. The Hamiltonian used to model the incomplete shell of $3d^4$ electrons in the transition-metal manganese atom consists of the crystal field, spin-orbit, spin-spin, and the Zeeman terms. The 25×25 Hamiltonian matrix was found by using an uncoupled angular momentum basis set and diagonalized numerically. The structure of the field-dependent energy levels is shown. The energy eigenvalues were used to compute the magnetization of the system. For a sample with $x=6.6\%$ at temperatures from 50 to 400 K and fields up to 7 T agreement with experiment was excellent with only one adjustable parameter, the spin-orbit coupling constant, λ. At low temperatures the interaction of the Mn atoms lowers the magnetization of the system relative to the singlet model that does not incorporate these interactions. For temperatures <50 K we modeled the Mn pair interactions by introducing a nearest-neighbor antiferromagnetic exchange interaction with an effective exchange coefficient; this brings the agreement with experiment down to about 20 K. For temperatures below 20 K the spin-glass-like cusp in the experimental data at 11 K suggests that the longer-range Mn interactions become significant. The good agreement of our results with experiment over a wide region of parameter space is a significant step toward understanding the magnetic properties of this new class of DMS.

DOI: 10.1103/PhysRevB.65.195211 PACS number(s): 75.50.Pp, 71.70.Ch, 71.70.Ej, 75.10.Dg

I. INTRODUCTION

Recently a new class of diluted magnetic semiconductors (DMS) have been fabricated in the laboratory.[1–3] These materials have the composition, $A^{III}{}_{1-x}M_xB^{VI}$ where $A^{III}B^{VI}$ is a III-VI semiconductor and M is a transition-metal atom. In the past few years[4] considerable interest in these materials has arisen because of their potential for photoelectronic applications and their nonlinear optical properties.

The focus of this paper is the covalently bonded III-VI semiconductor, GaS. Although there have been a few experimental studies, including measurements of thermal conductivity,[5] growth of films and multilayers,[6,7] and a measurement[1] of the magnetization of GaS containing substitutional Mn, there has been comparatively little theoretical work on III-VI DMS. In this paper we report on a theoretical investigation of the magnetization of a III-VI DMS, namely, $Ga_{1-x}Mn_xS$, concentrating on the limit $x<0.07$. In this limit one would anticipate the effects of any possible Mn interactions beyond a nearest-neighbor superexchange to be negligible except at low temperatures where a cusp has been observed that is reminiscent of the spin-glass transitions in II-VI (Refs. 8, 9) DMS systems. Using a Hamiltonian that is appropriate to the symmetry of the III-VI systems we have built on the theory used in investigations of the tetrahedral II-VI DMS (Refs. 10–12) systems. We calculate the magnetization of the two-dimensional $Ga_{1-x}Mn_xS$ system by performing an exact numerical diagonalization of the Hamiltonian matrix. The formulation was checked by comparing our results to both theoretical and experimental results for a number of the earlier tetrahedral and Wurtzite II-VI systems. On further comparison of the calculated magnetization to recent III-VI measurements it is found that Mn with an outer $3d^4$ configuration give magnetization results that are in good agreement with experiment for temperatures from 50 to 400 K in fields up to 7 T. Agreement is extended to 20 K by introducing a nearest-neighbor antiferromagnetic exchange interaction between the Mn spins.

This paper is a significant step toward modeling the magnetic behavior of the new class of III-VI DMS. We have made several assumptions in this model. One assumption is the point-ion approximation of crystal-field theory, which replaces the covalently bonded atoms by point ions. This approximation keeps the correct symmetry but does introduce errors since the bonds are covalent and not ionic.[25] The errors introduced by this assumption are corrected either by using an adjustable parameter in the model, as we have done, or, if optical data are available, using them to get the exact crystal-field energy-level splittings. From the point-ion standpoint, the emphasis in this paper is more on the magnetic properties of the local electronic d states of the substitutional transition-metal atoms rather than the band-structure levels of the pure semiconductor crystal. An additional assumption, made throughout most of the paper, is the singlet approximation that postulates the magnetic spins of the substitutional transition-metal atoms are noninteracting. Nevertheless, in spite of these restrictions, the model reproduces the experimental data well for a wide region of temperatures and magnetic fields.

II. MODEL HAMILTONIAN

The magnetic-field dependent energy levels of a system determine the magnetization of the material. We begin by

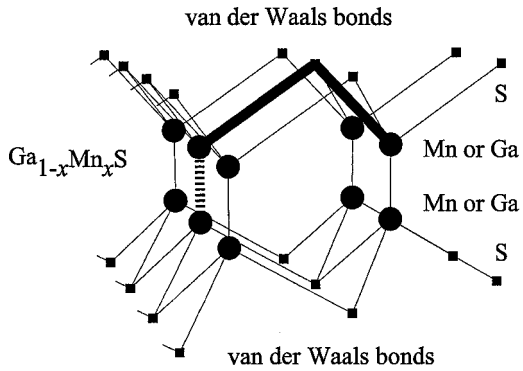

FIG. 1. The geometry of the GaS layered semiconductor modeled in this paper. The transition-metal atom, Mn, substitutes for the Ga atom with probability x. Shown is one portion of a four-atom-thick layer. Neighboring layers are coupled via the van der Waals interaction. The bold and dashed lines in the figure illustrate possible channels of exchange interactions between the neighboring Mn atoms. These interactions lie outside the singlet model.

finding the energy levels of a transition-metal atom, Mn, placed substitutionally in a crystal with an applied magnetic field, **B**. The substitutional Mn atom is bonded to its four neighbors via covalent bonds. The energy levels of the *d* electrons of the Mn atom are altered by the crystal field produced by its neighbors. Within the point-ion approximation one replaces these neighbors and their covalent bonds with point ions. The Mn *d* electron energy levels are then determined by, among other variables, the crystal symmetry, distance between ions, bond angles, and the oxidation states of the ions in the crystal. Such bonding properties must be found from experiment. The bond lengths have been measured[13] for a similar material, GaSe, and these values were used in this paper. Our results were not very sensitive to these variables and consequently, using the GaSe data should not introduce significant error.

$Ga_{1-x}Mn_xS$ consists of van der Waals coupled four-atom-thick layers with a manganese ion substituting for a gallium ion with a probability *x*. The manganese ion resides at the center of a distorted tetrahedron with three Mn-S covalent bonds (bond length $R \cong 2.473$ Å in GaSe) and one Mn-Ga covalent bond (bond length $R' \cong 2.388$ Å in GaSe). We denote the angle between the Mn-Ga bond and each of the Mn-S bonds θ (in the ideal tetrahedral case $\theta = 109.5°$ and this is the value we used). The geometry is illustrated in Fig. 1. The Ga-S bonds are partially covalent with the sulfur atoms in oxidation state $Z = -2$ and the gallium atoms in oxidation state $Z' = +2$.

One can reasonably postulate two candidate oxidation states of the substitutional manganese, either +2 or +3. We would expect Mn^{+2} to behave as a nearly free ion with a $3d^5$ outer electron configuration and a ^6S ground-state term. Consequently, the effects of the crystal field, spin-orbit, and spin-spin coupling should be quite small in Mn^{+2} as was found in the II-VI DMS systems.[8,9] The magnetization is simply given by the Brillouin function. In contrast, Mn^{+3} has a $3d^4$ outer electron configuration and a ^5D ground-state term according to Hund's rules. The crystal field should exert a strong influence on the $3d$ energy levels of the Mn^{+3} ion. The two $3d$ valence configurations of Mn have different magnetic moments and therefore behave dramatically different as will be illustrated below.

The Hamiltonian for an isolated transition-metal ion in a crystal is of the form[14]

$$H = H_{\text{free-ion}} + H_{\text{crystal}} + H_{\text{spin-orbit}} + H_{\text{spin-spin}} + H_{\text{Zeeman}}, \tag{1}$$

where $H_{\text{free-ion}}$ is the Hamiltonian of the free ion [for the $3d^4$ Mn ion, $(2L+1)(2S+1) = 25$-fold degenerate ground term, ^5D], the spin-orbit Hamiltonian,

$$H_{\text{spin-orbit}} = \lambda \mathbf{L} \cdot \mathbf{S}, \tag{2}$$

the spin-spin Hamiltonian,

$$H_{\text{spin-spin}} = -\rho[(\mathbf{L}\cdot\mathbf{S})^2 + \tfrac{1}{2}(\mathbf{L}\cdot\mathbf{S}) - \tfrac{1}{3}L(L+1)S(S+1)], \tag{3}$$

and the Zeeman Hamiltonian,

$$H_{\text{Zeeman}} = \mu_B(\mathbf{L} + 2\mathbf{S})\cdot\mathbf{B}. \tag{4}$$

In the above equations, $\mathbf{L}(\mathbf{S})$ is the total orbital(spin) operator for the *d* electrons of the transition metal ion, **B** the applied magnetic field, μ_B the Bohr magneton, $L(S)$ the total orbital(spin) quantum numbers ($L = S = 2$, for the ground term) and from Ref. 14 we find for the Mn ion the values $\lambda = 88\ \text{cm}^{-1}$ and $\rho = 0.18\ \text{cm}^{-1}$. It should be noted, however, the value used for λ was $21\ \text{cm}^{-1} \pm 5$ cm rather than the $88\ \text{cm}^{-1}$ value. Reference 14 gives values of λ appropriate to a *free ion* rather than an ion in a matrix and as pointed out there, the free ion values are usually substantially *larger* than those for ions in a crystal. Consequently, for this reason and reasons stated below, λ was used as a fitting parameter.

The crystal-field term of the Hamiltonian in Eq. (1) is found by expanding the Coulomb potential for the interaction of the *d* electrons, positions $\{\mathbf{r}_i\}$, with the neighboring crystal point ions, positions $\{\mathbf{R}_j\}$, in spherical harmonics.

$$H_{\text{crystal}}(\mathbf{r}_i, \{\mathbf{R}_j\}) = -e\sum_i \sum_j \frac{eZ_j}{|\mathbf{R}_j - \mathbf{r}_i|} = \sum_i \sum_l \sum_{m=-l}^{l} A_l^m r_i^l Y_l^m(\theta_i, \phi_i), \tag{5}$$

where

$$A_l^m \equiv \frac{4\pi e^2}{2l+1} \sum_j \frac{Z_j Y_l^{m*}(\theta_j, \varphi_j)}{R_j^{l+1}}.$$

Equation (5) assumes the covalent bonds between the Mn atom and its Ga and S neighbors may be approximated as ionic bonds with the charge of the neighboring Ga and S ions possessing spherical symmetry. Because of this approximation optical data are often used to determine the energy-level splitting by the crystal field (see Ref. 14, p. 394). In the absence of optical data for $Ga_{1-x}Mn_xS$ we have used the crystal-field levels based on Eq. (5), and we used the spin-orbit coupling constant λ as a fitting parameter.

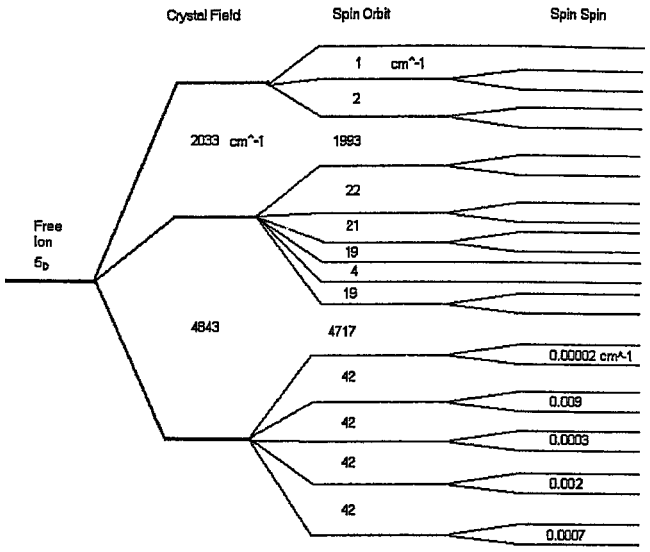

FIG. 2. Energy-level diagram for $Ga_{1-x}Mn_xS$ assuming Mn^{3+} and C_{3v} symmetry. The numbers refer to the energy gap in units of cm^{-1}.

The coordinate axes we used have the origin at the Mn ion, the *x* axis coming out of the page (parallel to the two-dimensional layers) and the *z* axis along the Mn-Ga bond (perpendicular to the layers). We have oriented the crystal relative to our axes so that the third ($j=3$) S ion is behind the page residing in the *x*-*z* plane. With this arrangement, the sulfur ions ($j=1,2,3$) have positions in spherical coordinates ($R=R_1=R_2=R_3$, $\theta_1=\theta_2=\theta_3=109.5°$, and $\phi_1=60°$, $\phi_2=180°$, and $\phi_3=300°$), and oxidation state $Z=Z_1=Z_2=Z_3$, while the Ga ion has position ($R_4=R'=$length of the Mn-Ga bond, $\theta_4=0$, $\phi_4=0$) and oxidation state $Z_4=Z'$. Because of the crystal symmetry[10] (point-group symmetry C_{3v} at the transition-metal site) only the following A_l^m's are nonzero: A_2^0, A_4^0, $A_4^3=-A_4^{-3}$. We find for the operator equivalent crystal field Hamiltonian,[15,16]

$$H_{\text{crystal}}=b[3L_z^2-L(L+1)]+a\{35L_z^4+[25-30L(L+1)]L_z^2+3L^2(L+1)^2-6L(L+1)\}-d\{L_z,L_+^3+L_-^3\}. \quad (6)$$

Here $L_\pm\equiv L_x\pm i\,L_y$ and L_x, L_y, and L_z are the components of the total orbital angular momentum operator along the Cartesian axes, *x*, *y*, and *z*. In Eq. (6), { } represents an anticommutator and the coefficients are given by

$$b\equiv A_2^0\langle\alpha\rangle\langle r^2\rangle\sqrt{5/16\pi},$$

$$a\equiv A_4^0\langle\beta\rangle\langle r^4\rangle\sqrt{9/256\pi},$$

$$d\equiv A_4^3\langle\beta\rangle\langle r^4\rangle\sqrt{1.23/\pi},$$

where for Mn^{+3} (Ref. 14), $\langle\alpha\rangle=2/21$, $\langle\beta\rangle=-2/63$, $\langle r^2\rangle=1.286$ a.u. (atomic units), and $\langle r^4\rangle=3.466$ a.u.

The matrix representation of the Hamiltonian was obtained using the "uncoupled" angular momentum basis states, $|LSM_LM_S\rangle$. In the case of Mn with $3d^4$, $L=S=2$ and both M_L and $M_S=0,\pm1,\pm2$. The full Hamiltonian matrix has dimensions 25×25. However, in the case of Mn with $3d^5$, $L=0$, $S=5/2$, $M_L=0$, and $M_S=\pm1/2,\pm3/2,\pm5/2$ and the Hamiltonian matrix is 6×6 because only the Zeeman term contributes to the full Hamiltonian. The diagonalization of the Hamiltonian was performed numerically.

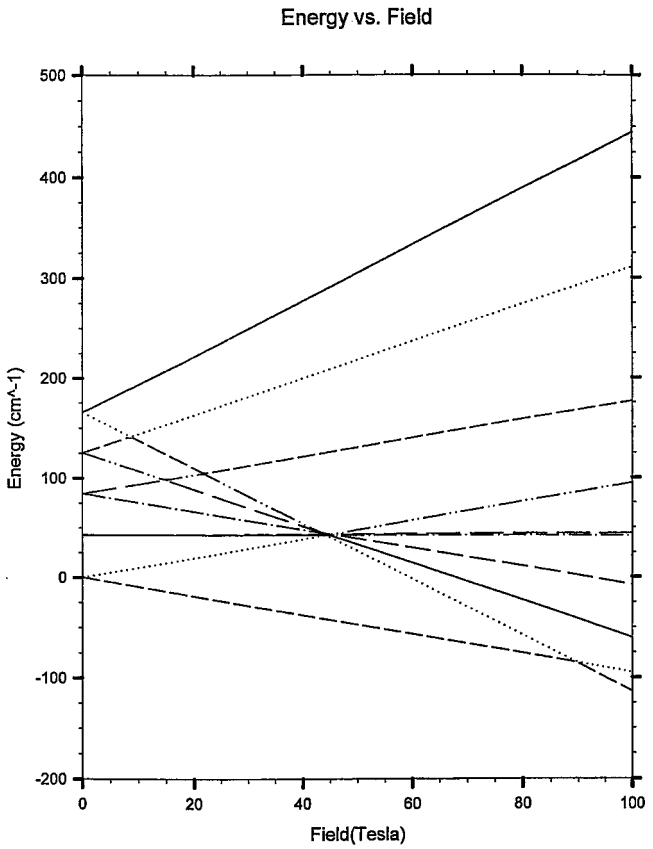

FIG. 3. The dependence on magnetic field of the ten lowest energy levels of Fig. 2. The magnetic field is along the *z* axis. The ground-state energy has been subtracted from each of the levels. The slope of each of these curves gives the magnetic dipole moment of the ion for that state. The presence of magnetization "steps" in the magnetization versus field plot would not be manifest until 90 T where two low energy levels cross. This field is rather large and may be difficult to produce in the laboratory at this time.

III. RESULTS

We first performed a series of benchmark tests on several II-VI DMS systems. The II-VI DMS, $Cd_{1-x}Fe_xTe$ has tetrahedral symmetry. Upon increasing the values of *a*, *b*, and *d* in our crystal potential we found the energy levels versus field for the lowest ten levels to be in excellent agreement with previous workers'[17–19] results. Our magnetization versus field results for $Cd_{1-x}Fe_xTe$ matched those of Fig. 8 of Ref. 20 for the magnetic field in the [111] direction (our $\theta_B=0$). As a more robust test, we considered the Wurtzite II-VI DMS system, $Cd_{1-x}Fe_xSe$. With values for *a*, *b*, and *d* in our crystal potential expression taken from optical measurements[21] we obtained magnetization versus field results matching those in Fig. 3 of Ref. 22.

Returning to $Ga_{1-x}Mn_xS$, initially we calculated the magnetization assuming $3d^5$ for the Mn ion as was the case in

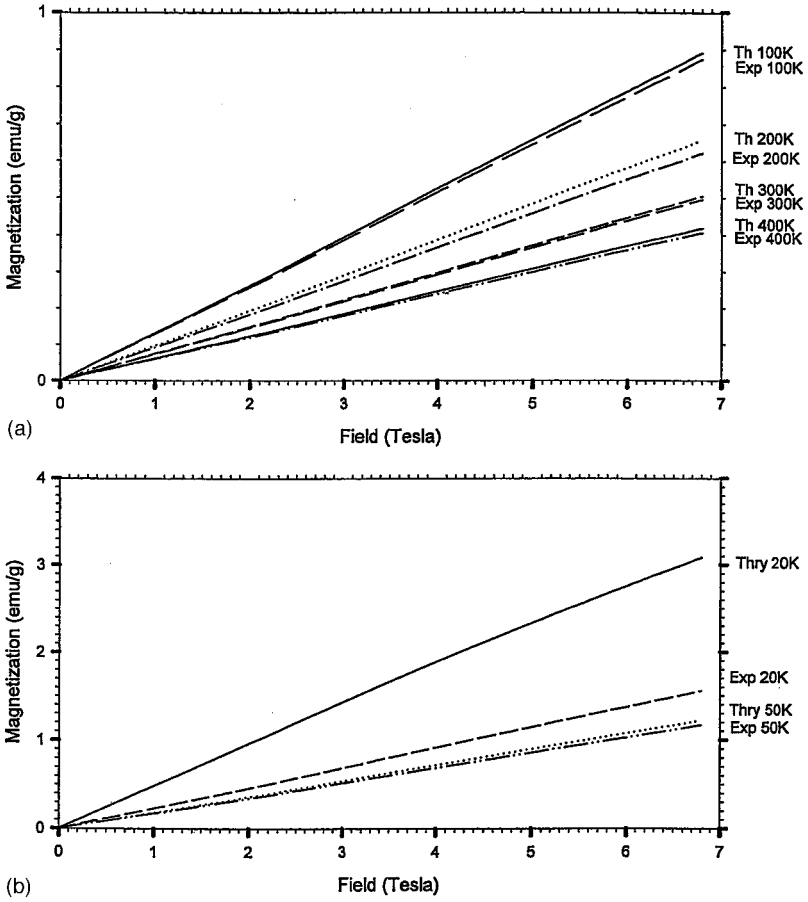

FIG. 4. (a) Magnetization versus field for $Ga_{1-x}Mn_xS$ with field along the z axis. The magnetization is found at four temperatures, 100, 200, 300, and 400 K, and assumes ionization state Mn^{3+}. Shown also is the experimental magnetization. The nominal concentration of Mn is $x=6.6\%$. (b) Same as Fig. 3(a) except at the two temperatures, 50 and 20 K. The disagreement with experiment at the lower temperature points to the possibility of Mn-Mn interactions.

the II-VI's. The calculated magnetization is unreasonably *larger* than the experimental values, leading us to consider the $3d^4$ Mn configuration.

The energy-level diagram for Mn $3d^4$ case is shown in Fig. 2. The numbers in Fig. 2 give the spacing of the levels in cm^{-1}; the diagram is not to scale. The crystal-field interaction splits the 25-fold degenerate free ion term into a fivefold degenerate and a tenfold degenerate set of higher energy states and a ground state of tenfold degeneracy. The spin-orbit interaction removes some of these degeneracies as shown in the figure. The spin-spin term further split these states by a small amount (<0.01 cm^{-1}) lifting all remaining degeneracies as can be seen on the far right of Fig. 2. Of primary interest are the ten low-lying states since they largely determine the magnetization.

Figure 3 is a graph of these ten lowest energy levels as a function of field. For a given energy level, the level contributes a magnetic moment given by the slope of the curve. More specifically, the energy levels determine the magnetization according to,

$$M(T,B)=-\frac{n(x)}{Z}\sum_{i=1}^{N} e^{-\beta E_i}\frac{\partial E_i}{\partial B}. \tag{7}$$

In Eq. (7), $\beta=1/k_BT$ (with k_B the Boltzmann constant), Z is the partition function,

$$Z(T,B)=\sum_{i=1}^{N} e^{-\beta E_i}, \tag{8}$$

where N is the number of energy levels ($N=25$ for Mn with $3d^4$) and $n(x)$ gives the number of Mn ions per unit mass of the sample for concentration x, that is,

$$n(x)=xN_A/[(1-x)M_{\mathrm{Ga}}+xM_{\mathrm{Mn}}+M_{\mathrm{S}}], \tag{9}$$

where M is the atomic mass and N_A is Avogadro's number.

The magnetization versus field at several constant temperatures is shown in Fig. 4 with good agreement with experiment from about 50 to 400 K. Figure 5 is a graph of the magnetization versus temperature with a constant magnetic field of 0.1 and 1 T. The agreement of theory with experiment is good for temperatures above about 50 K. The deterioration in agreement below 50 K is likely due to Mn-Mn interactions that are not accounted for in the singlet model. In fact, the experimental data[1] show a cusp at about 11 K, which is reminiscent of the spin-glass transitions seen in II-VI DMS systems.

In an effort to extend the agreement with experiment to temperatures below 50 K an additional term was added to the Hamiltonian to model the Mn-Mn interactions. We introduced a Heisenberg antiferromagnetic interaction between nearest-neighbor Mn ions with an effective coupling constant $J_{\mathrm{eff}}/k_b\cong-50$ K, the temperature where the singlet model

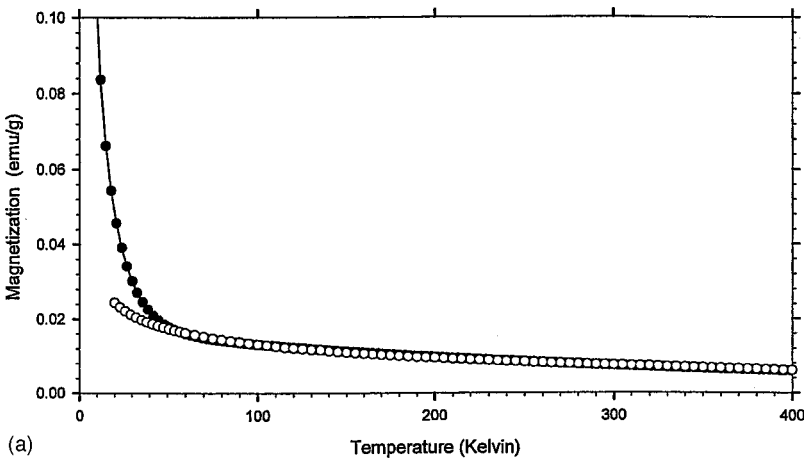

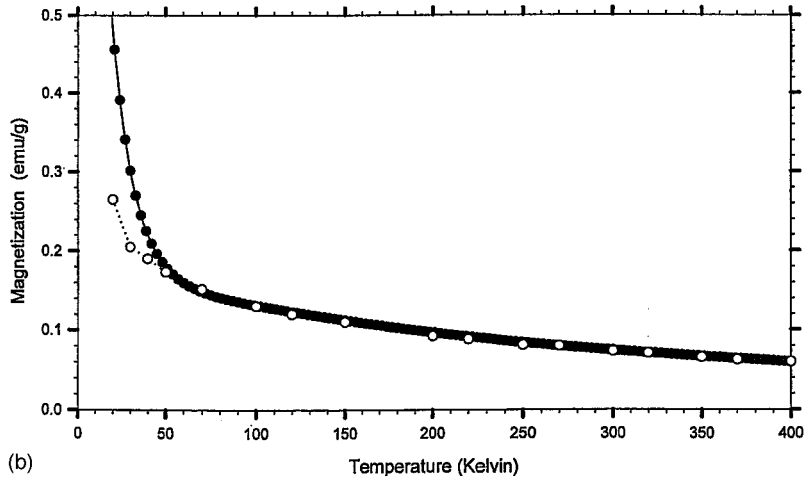

FIG. 5. (a) Magnetization versus temperature for $Ga_{1-x}Mn_xS$ with field of 0.1 T along the z axis. The nominal concentration of Mn is $x = 6.6\%$. The magnetization was calculated assuming singlet Mn^{3+}. The open circles represent the experimental results while filled circles are for the theory. (b) Same as Fig. 4(a) except the applied field is 1 T.

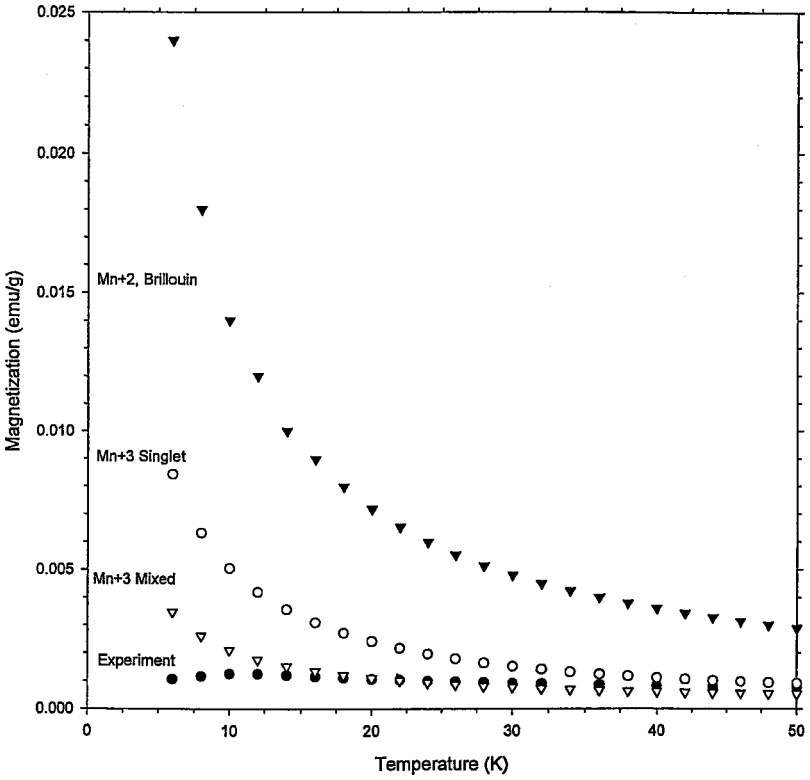

FIG. 6. Magnetization versus temperature of $Ga_{1-x}Mn_xS$ in an applied magnetic field of 0.005 T. The value of x is 0.066. The theoretical curves are: Mn^{+2} $3d^5$ (Brillouin), Mn^{+3} $3d^4$ (singlet), and singlets and doublets of Mn^{+3} (mixture). The experimental data are from Ref. 1.

suggests pairing becomes important. For two Mn ions (a ''doublet'') with total angular momentum operators, $\mathbf{J}_1$ and $\mathbf{J}_2$, the coupling takes the form,

$$H_{\text{doublet}} = -J_{\text{eff}}\mathbf{J}_1 \cdot \mathbf{J}_2 + g\mu_B B(J_{1z} + J_{2z}). \tag{10}$$

The energy eigenvalues of the pair are,[23]

$$E_{\text{doublet}} = -\frac{J_{\text{eff}}}{2} J_T(J_T+1) + g\mu_B B J_{Tz}, \tag{11}$$

where $g=2$ and $J_T = J_1 + J_2, \ldots, |J_1 - J_2| = 8,...,0$ is the total angular momentum quantum number of the two coupled Mn ions and for a given value of J_T, $J_{Tz} = J_T, \ldots, -J_T$. The total magnetization when only singlet and doublet Mn ions are present with probabilities p and $(1-p)$, respectively, we find by averaging,[20]

$$M_{\text{mixed}} = pM_{\text{singlet}} + (1-p)M_{\text{doublet}}. \tag{12}$$

The doublet magnetization was found by using the same expression for magnetization as in Eq. (7), except we divided that expression by two and used the doublet eigenvalues.

Results are shown in Fig. 6. Included in this figure is the Mn with $3d^5$, a Brillouin function, which is unreasonably *larger* than the experimental magnetization, a curve that assumes only Mn with $3d^4$ singlets, and the Mn with $3d^4$ ''mixed'' curve that includes both singlets and doublets with magnetization computed from Eq. (12). Assuming the manganese atoms substitute for the gallium atoms in a random fashion then the probability Mn is a singlet is given by the expression,[2] $p=(1-x)^{13}$, where x is the concentration of manganese. Clearly, the mixed model improves the agreement of the singlet model with experiment by lowering the singlet magnetization because of the antiferromagnetic coupling of the ions; agreement is good all the way to about 20 K.

IV. CONCLUSION

The present work extends the calculation of the magnetization of II-VI DMS to the new class of layered III-VI DMS systems. The Hamiltonian used to represent the *d* electrons of the transition-metal ion consists of crystal field, spin-orbit, spin-spin, and Zeeman contributions. The eigenvalues of this Hamiltonian were used to find the magnetization of the system. In the absence of optical data that could be used to adjust the crystal potential levels, we used the first-principles crystal potential in the point-ion approximation and treated the spin-orbit coupling parameter, λ, as a fitting parameter. The good agreement of the singlet results with experiment over the wide temperature range of 50 to 400 K in fields from 0 to 7 T suggests that the model captures much of the physics of the magnetization of the $Ga_{1-x}Mn_xS$ material.

Our conclusion that the Mn with a $3d^4$ electron configuration more closely coincides with the experimental magnetization data than the $3d^5$ configuration used in the II-VI DMS points out an interesting contrast between II-VI and III-VI DMS systems. In the II-VI tetrahedral systems the substitutional transition-metal atom bonds to four identical atoms, whereas in the III-VI layered systems studied in this paper the Mn also bonds to four atoms but only three are S atoms and the fourth is a Ga atom. In undoped GaS the Ga atom is in the $+2$ oxidation state. However, in $Ga_{1-x}Mn_xS$ the substitutional Mn does not acquire a $+2$ oxidation state but rather a $+3$ state. This is because the Mn-Ga bond is between atoms of slightly different electronegativity[24] [the electronegativity of Mn is slightly smaller (1.5) than that of the Ga atom (1.6)]. The electrons in the covalent bond between the substitutional Mn atom and its Ga neighbor (see Fig. 1) would be concentrated slightly closer to the Ga atom, and therefore in the point-ion approximation the Mn ion would have an oxidation state $+3$ with outer shell configuration $3d^4$. Consequently, the magnetic behavior of the Mn^{+3} ion with outer shell configuration $3d^4$ in the layered III-VI DMS $Ga_{1-x}Mn_xS$ is in sharp contrast to the extensively investigated Mn^{+2} ion with outer shell configuration $3d^5$ in the II-VI DMS.

Going beyond the singlet model we found that modeling the Mn ions as pairs using a simple nearest-neighbor antiferromagnetic interaction brought the agreement with experiment down to about 20 K. Consequently, this work shows promise as a model that can be extended to incorporate Mn interactions with longer-range magnetic coupling that becomes significant for temperatures <20 K. To this end, calculations are underway to extend the doublet model by including Mn triplets, to include the effects of magnetic anisotropy in $Ga_{1-x}Mn_xS$, and to compute the magnetic heat capacity.

ACKNOWLEDGMENTS

This research was supported by Cottrell Science Awards, CC4845 and CC4719 of Research Corporation, NSF Grants Nos. DMR-99-72196, DMR-99-75887, DMR-01-02699, and ECS-01-29853, Purdue University Academic Reimbursement Award and UNF Research Grants.

[1] T. M. Pekarek, M. Duffy, J. Garner, B. C. Crooker, I. Miotkowski, and A. K. Ramdas, J. Appl. Phys. **87**, 6448 (2000).

[2] T. M. Pekarek, B. C. Crooker, I. Miotkowski, and A. K. Ramdas, J. Appl. Phys. **83**, 6557 (1998).

[3] T. M. Pekarek, C. Fuller, J. Garner, B. C. Crooker, I. Miotkowski, and A. K. Ramdas, J. Appl. Phys. **89**, 7030 (2001).

[4] D. Errandonea, A. Segura, V. Munoz, and A. Chevy, Phys. Rev. B **60**, 15 866 (1999).

[5] M. A. Alzhdanov, M. D. Nadzhafzade, and X. Yu. Seidov, Phys. Solid State **41**, 20 (1999).

[6] A. B. M. O. Islam, T. Tambo, and C. Tatsuyama, J. Appl. Phys. **85**, 4003 (1999).

[7] M. Budiman, T. Okamoto, A. Yamada, and M. Konagai, Jpn. J. Appl. Phys., Part 1 **37**, 5497 (1998).

[8] *Diluted Magnetic Semiconductors*, edited by Mukesh Jain (World Scientific, Singapore, 1991).
[9] See also, *Semiconductors and Semimetals*, edited by J. K. Furdyna and J. Kossut (Academic, Boston, 1988), Vol. 25.
[10] Murielle Villeret, S. Rodriguez, and E. Kartheuser, Phys. Rev. B **41**, 10 028 (1991).
[11] Murielle Villeret, Sergio Rodriguez, E. Kartheuser, Angela Camacho, and Luis Quiroga, Phys. Rev. B **44**, 399 (1991).
[12] T. M. Pekarek, J. E. Luning, I. Miotkowski, and B. C. Crooker, Phys. Rev. B **50**, 16 914 (1994).
[13] S. Jandl, J. L. Brebner, and B. M. Powell, Phys. Rev. B **13**, 686 (1976); see also, *Progress in Crystal Growth and Characterization of Materials*, edited by J. B. Mullin (Pergamon, New York, 1994), p. 276.
[14] *Electron Paramagnetic Resonance of Transition Ions*, edited by A. Abragam and B. B. Bleaney (Oxford University Press, New York, 1971).
[15] D. Scalbert, J. Cernogora, A. Mauger, C. Benoit a la Guillaume, and A. Mycielski, Solid State Commun. **69**, 453 (1989).
[16] J. Patrick Mahoney, Chun C. Lin, William H. Brumage, and Franklin Dorman, J. Chem. Phys. **53**, 4286 (1970).
[17] C. Testelin, A. Mauger, C. Rigaux, M. Guillot, and A. Mycielski, Solid State Commun. **71**, 923 (1989).
[18] Murielle Villeret, Sergio Rodriguez, and E. Kartheuser, Phys. Rev. B **43**, 3443 (1991).
[19] Glen A. Slack, S. Roberts, and J. T. Vallin, Phys. Rev. **187**, 511 (1969).
[20] C. Testelin, C. Rigaux, A. Mauger, and A. Mycielski, Phys. Rev. B **46**, 2193 (1992).
[21] M. K. Udo, Murielle Villeret, I. Miotkowski, A. J. Mayur, A. K. Ramdas, and S. Rodriquez, Phys. Rev. B **46**, 7459 (1992).
[22] A. Twardowski, K. Pakula, I. Perez, P. Wise, and J. E. Crow, Phys. Rev. B **42**, 7567 (1990).
[23] Y. Shapira, J. Appl. Phys. **67**, 5090 (1990).
[24] See, Table 6–4, Linus Pauling, *General Chemistry* (Dover, New York, 1970), p. 182.
[25] M. Schluter and M. L. Cohen, Phys. Rev. B **14**, 424 (1976).